J. Membrane Biol. 1, 431 – 458 (1969)

Measurement of Axonal Membrane Conductances and Capacity by Means of a Varying Potential Control Voltage Clamp

YORAM PALTI* and WILLIAM J. ADELMAN, JR.

Department of Physiology, University of Maryland, School of Medicine, Baltimore, Maryland 21201, and Marine Biological Laboratory, Woods Hole, Massachusetts 02543

Received 18 August 1969

Summary. A new mode of voltage clamping in the squid giant axon is introduced and its advantages are analyzed, tested, and utilized to investigate membrane conductances and capacity. This method replaces the constant command potentials of the standard voltage clamp with potentials which vary with time. Some of the advantages in using the varying potential clamp are: (1) slowly varying potentials generate practically pure I_K; (2) rapidly varying potentials generate practically pure I_{Na}; (3) triangular waves generate, under proper conditions, pure capacity currents and easy-to-analyze leakage currents; (4) the method gives direct, on-line display of sodium or potassium I-V characteristics within milliseconds; (5) it enables rapid and accurate E_{Na} and E_K determinations; and (6) it enables simple and accurate determination of C_m. The method was utilized to study the effects of various ions on membrane conductances and the effects of ionic composition, ionic strength, and temperature on membrane capacity. Membrane capacity was found to be practically independent of frequency in the 200 to 2,000 Hz range. Replacement of external sodium by Ca^{++}, by impermeable $Tris^+$, or even by dextrose or sucrose (low ionic-strength solutions) had negligible effects on C_m. C_m showed a small, positive temperature coefficient of 1.39% per °C in the 3 to 21 °C range, and little change with temperature in the 20 to 40 °C range. Above 40 °C, both C_m and g_L increased considerably with temperature.

Since its introduction by K. S. Cole in 1949, the voltage clamp technique has become the accredited method for studying the ionic currents and conductances associated with the activity of excitable membranes. Basically, the technique involves holding the membrane potential, E_m, at one prefixed value and then stepping it to another. The change in potential is achieved by means of an electronic feedback circuit which regulates E_m by driving an appropriate current through the membrane so that E_m matches a given command potential. In contrast to the natural excitation process, where

* Permanent address: Department of Physiology, The Hebrew University, Hadassah Medical School, Jerusalem, Israel.

both the membrane potential and the current change as functions of time, an adequate step voltage clamp results in E_m being known and constant with time and uniform over a given area of membrane. Thus, from the measured membrane currents, I_m, associated with various E_m steps, one can directly determine the membrane conductance changes as a function of potential and time. Based on voltage clamp measurements, the total membrane current has been fractionated into a number of ionic components by means of variations in the ionic composition of both the external (Hodgkin & Huxley, 1952*a*, *b*, *c*) and the internal (Chandler & Meves, 1965) media. On the basis of these results, Hodgkin and Huxley formulated mathematical functions by means of which both the behavior of nerve under a variety of conditions and the generation of the nerve impulse can be reconstructed (Hodgkin & Huxley, 1952*c*; Adelman & Palti, 1969). Although the analysis of results obtained by means of this powerful method continues to yield information contributing to the understanding of the mechanisms underlying excitable membrane activity, a new approach to the voltage clamp technique has recently been described (Palti & Adelman, 1969). To control membrane potential, the method utilizes a command voltage which varies as a function of time. Two types of variation were applied: sine waves and triangular waves. In this new voltage clamp mode, the voltages are well-defined variables which offer special analytical and experimental advantages. By clamping the axon membrane to selected continuously varying voltages, one can obtain immediate membrane current separations, membrane current-voltage relationships over a wide range of voltages, membrane kinetic parameters, direct determination of membrane capacity, etc. The triangular-wave-mode variable-potential voltage clamp is analogous to the ramp clamp described in a preliminary report by Fishman and Cole (1969).

This report presents an analytical and experimental evaluation of the method. It also includes new experimental data obtained by means of this method.

Methods

Experimental

Giant axons of the squid, *Loligo pealei*, were isolated and placed in a cell perfused with artificial sea water (ASW) or various other solutions (*see* Table 1). Membrane potential was monitored by a 3 M KCl-filled microelectrode located at the inner surface of the axon membrane. E_m was controlled by passing a current between a platinized axial electrode and external electrodes as previously described (Adelman & Palti, 1969). The electronic voltage control system used differed from those previously described in that the standard pulse or step command potential could be substituted by a con-

tinuously varying command potential. These potentials, sine or triangular waves, were generated by a Wavetek model 114 Voltage Controlled Waveform Generator. Each axon was voltage clamped by means of both the standard step-clamp procedure and the continuously varying potential clamp procedure. In the latter procedure, the membrane potential was usually first clamped and held constant at the resting value, E_H, and then forced to vary with time. The first half-cycle was usually in the hyperpolarizing direction and the next in the depolarizing direction (*see* Figs. 3 & 10). A single or as many as 100 complete cycles were used for each frequency and amplitude. The two functions used to command the voltage change in addition to the step command were:

$$E_m = E_H + E_0 \quad \text{sine} \quad \omega t, \tag{1}$$

and

$$E_m = E_H + A t \tag{2}$$

where E_0 is the potential measured from E_H to the peak, $\omega = 2\pi f$, f is the frequency of the wave, and A is a slope coefficient which changes its sign in pace with sine ωt. E_0 was varied from zero to ± 160 mV and the frequency from 10 to 5×10^3 Hz.[1] The frequency response of the electronic system was linear and practically free of distortion throughout the frequency range. The membrane potentials and currents were recorded on a Tektronix 565 oscilloscope. Each axon was clamped to the two oscillatory potentials as well as to conventional step potentials. Results obtained with oscillatory clamps were compared to those obtained with pulse clamps. The total ionic membrane current was separated into I_{Na}, I_K and I_L components by substituting $Tris^+$ for Na^+ and by varying $[K_0^+]$ (*see* Table 1). In all, 10 axons were studied.

Analytical

The nerve membrane currents were calculated for both step and varying potential clamps with use of an IBM 360/44 digital computer. The computations were carried out using the following equations formulated by Hodgkin and Huxley (1952*c*) to describe the axon behavior:

$$I_m = C_m \, dE_m/dt + \bar{g}_{Na} m^3 h (E_m - E_{Na}) + \bar{g}_K n^4 (E_m - E_K) + g_L (E_m - E_L), \tag{3}$$

$$dm/dt = \alpha_m (1-m) - \beta_m m, \tag{4}$$

$$dn/dt = \alpha_n (1-n) - \beta_n n, \tag{5}$$

$$dh/dt = \alpha_h (1-h) - \beta_h h, \tag{6}$$

$$\alpha_m = -0.1 (E_m + 35) \Big/ \left(\exp \left[\frac{-(E_m + 35)}{10} \right] - 1 \right), \tag{7}$$

$$\beta_m = 4 \exp \left[\frac{-(E_m + 60)}{18} \right], \tag{8}$$

$$\alpha_n = -0.01 (E_m + 50) \Big/ \left(\exp \left[\frac{-(E_m + 50)}{10} \right] - 1 \right), \tag{9}$$

$$\beta_n = 0.125 \exp \left[\frac{-(E_m + 60)}{80} \right], \tag{10}$$

[1] Note that Fourier analysis of triangular waves (Speigel, 1963) indicates that the contribution of frequencies above the third harmonic is negligible.

$$\alpha_h = 0.07 \exp\left[\frac{-(E_m+60)}{20}\right], \tag{11}$$

$$\beta_h = 1\Big/\left(\exp\left[\frac{-(E_m+30)}{10}\right]+1\right). \tag{12}$$

For definition of the conductance parameters (m, n, h) and the rate constants (α and β), see Hodgkin and Huxley (1952*c*)[2]. The following modified relations (Adelman & Palti, 1969) were used to describe sodium conductance in high $[K_0]$:

$$\alpha_h = (0.126 - 0.065 \log[K_0]) \exp\left[\frac{-(E_m+60)}{27.4}\right], \tag{11'}$$

$$\beta_h = 1\Big/\left(\exp\left[\frac{-(E_m+36)}{9}\right]+1\right) + 0.01 \exp[-E_m \cdot B_{(k)}] \tag{12'}$$

where

$$B_{(k)} = [K_0]/(32.5[K_0]+185).$$

The values of E_{Na}, E_K, E_L, $\bar{g}_{Na}$, $\bar{g}_K$, and g_L were determined for each nerve as described by Hodgkin and Huxley (1952*a*, *b*). In computations carried out for the Hodgkin-Huxley nerve model, the following values were used (FitzHugh, 1960): $E_{Na} = 55$ mV, $E_K = -72$ mV, $E_L = -49.4011$ mV, $\bar{g}_{Na} = 120$ mmho/cm^2, $\bar{g}_K = 36$ mmho/cm^2 and $g_L = 0.3$ mmho/cm.[2] To solve I_m, I_K, I_{Na} and I_L as a function of potential and time, the initial values of m, n, and h (m_0, n_0, h_0) were calculated using relations

$$m_0 = m_\infty = \frac{\alpha_m}{\alpha_m + \beta_m} \tag{13}$$

where α_m and β_m are those computed from Eqs. (7) and (8) using the holding potential (which usually equaled the resting potential) for E_m. A similar computation was carried out for n_0 and h_0, using relationships analogous to those in Eqs. (9)–(13). Using Taylor series, the m, n, and h functions known for t_0 were calculated for $t_0 + \Delta t$. For example, using only the first term of the series, the relation for m would be:

$$m_{(t_0+\Delta t)} = m_0 + \Delta t \, dm/dt = m_0 + \Delta t [\alpha_m(1-m) - \beta_m m]. \tag{14}$$

For the continuous functions of the type with which we are dealing and for a sufficiently small element of time, Δt, the error introduced by ignoring the terms subsequent to the first, becomes negligible. By means of the Runga-Kutta (Ralston & Wilf, 1960) method, a sufficiently small element of time, Δt, was defined. On the basis of Eq. (14), together with the above calculated initial values of m_0, n_0 and h_0, and the proper E_m values (as computed from Eqs. (1) & (2) for any t), Eqs. (4)–(6) were solved for m, n and h at time, $t + \Delta t$.[3] By continuously repeating the same procedure, the consecutive

[2] Note that the original V notation was replaced by the currently used E_m or absolute potential scale.

[3] In the specific case of a step potential function, Eqs. (4)–(6) can be solved directly by analytical methods (Hodgkin & Huxley, 1952*c*) and the above procedure obviously becomes redundant.

changes in the parameters m, n and h for small increments of time were solved numerically. At each point in time, the calculated values of m, n, h and E_m were substituted in Eq. (3) and the total, as well as each individual membrane current, was thus solved as a function of potential and time.

The computed values of the m, n and h parameters and the total membrane currents were tabulated and plotted by the digital computer. The presented plottings were traced from the computer print-outs. As only one of ten or more of the computed points was plotted, and as the printer can only place symbols at some minimal fixed spacings, the plottings do not, at times, appear smooth even though the solutions were continuous and smooth.

Results

Analytical

Membrane Conductance Parameters and Currents. A typical example of the variations in the m, n and h parameters during a step voltage clamp is illustrated in Fig. 1. The record simulates the membrane behavior upon stepping the membrane potential from $E_H = -80$ mV to $E_p = 0$ mV. As expected from the Hodgkin-Huxley equations, upon membrane depolarization,

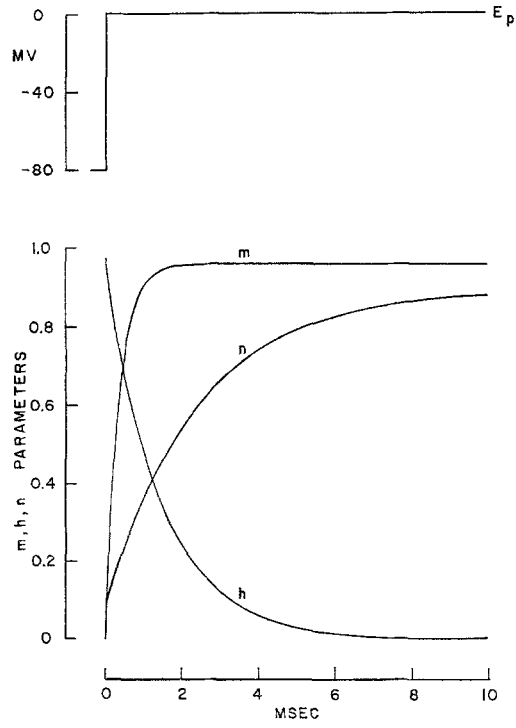

Fig. 1. Computer readout of Hodgkin-Huxley m, n and h parameter changes plotted as a function of time for a step change in membrane potential, E_m. E_m is changed from an initial holding potential $E_H = -80$ mV to $E_p =$ zero mV. Ordinate: m, n and h values. Abscissa: time in msec

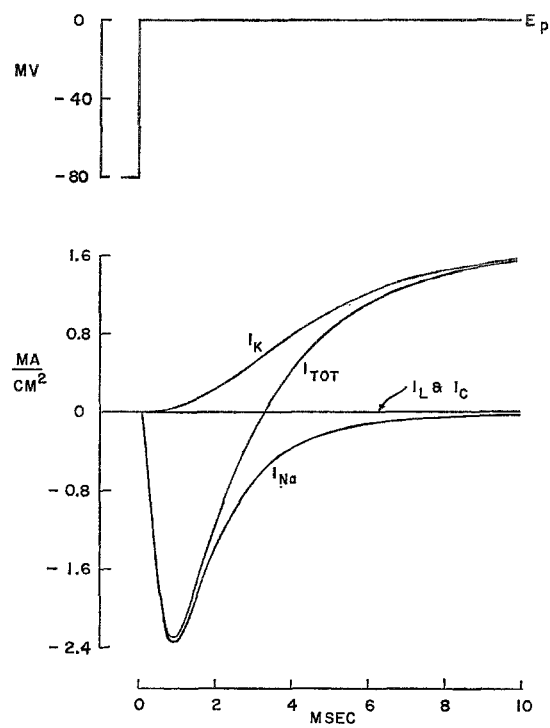

Fig. 2. Computer readout of the membrane currents generated in a voltage clamped axon upon stepping E_m from $E_H = -80$ mV to $E_p = 0$ mV. Ordinate: membrane currents; I_{Na}, I_K, I_{Cap}, I_{Leak} and I_T (total membrane current, I_m, in mA/cm²). Inward current plotted downward. The I_{Cap} line (capacity current) is the zero line. Leakage current is relatively small so that it is buried in the I_{Cap} line

m increases (to a value close to 1) with a fast time constant, τ_m, whereas h decreases and n increases with the appropriately slower time constants, τ_h and τ_n. Fig. 2 illustrates the corresponding membrane currents with the typical initial inward transient current and the steady state potassium current.

Fig. 3 illustrates the computed m, n and h parameters associated with a sinusoidal membrane potential change. In this particular case, the membrane potential was clamped to a low amplitude, $\Delta E_m = \pm 10$ mV ($E_0 = 10$ in Eq. (1)), sine wave of $f = 100$ Hz. Under these conditions, we see that the m, n and h parameters show a sine-like oscillation. However, each parameter is shifted to a different degree with respect to E_m. These well-behaved oscillations are typical of low potential swings where the response of the membrane can be considered approximately linear with voltage. The shifts are easy to understand on the basis of: (1) the known direction of response to potential of each of the parameters, and (2) the fact that in

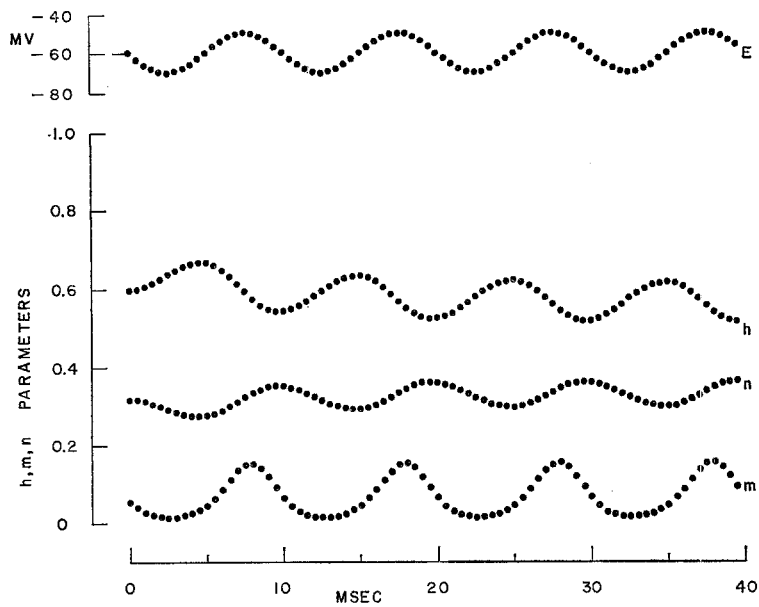

Fig. 3. Computer readout of Hodgkin-Huxley m, n and h parameters plotted as a function of time during a sine wave voltage clamp of f = Hz and amplitude of ± 10 mV, symmetric with respect to $E_H = -60$ mV. Prior to the beginning of the first oscillation (at the left hand of the figure), E_m was held at -60 mV. Ordinate: upper trace, membrane potential oscillation. Downward inflection hyperpolarization. Lower three traces, m, n and h parameters. Abscissa: time in msec. Note sine-like changes of parameters and downward trend of first few h cycles and upward trend of the corresponding n cycles

this clamp mode the responses are a function of both potential and time (i.e., they are determined also by the appropriate membrane time constants, τ_m, τ_n, and τ_h). Thus, in the above case, as $-E_m$ is increased (hyperpolarization), m decreases. Since τ_m is short as compared to f, m can easily follow the variations in E_m, and m is shifted 180° with respect to E_m. Like m, n decreases as $-E_m$ is increased. However, the response of n is relatively slow so that the net shift is more than 180°. On the other hand, h increases with $-E_m$ and, since τ_h is relatively slow, h lags behind E_m.

The well-behaved m, n and h parameter changes give way to more complex functions as E_0 is increased and the nerve conductances cease to behave linearly with potential. Fig. 4 illustrates the m, n and h changes during a cycle of low frequency (10 Hz), high amplitude ($\Delta E_m = \pm 120$ mV) membrane potential change. The parameters follow this low frequency, each saturating either at zero or at unity around the peak potential values. The resulting current is almost completely rectified (Fig. 5). There is practically no current throughout the hyperpolarizing half-cycle. At the

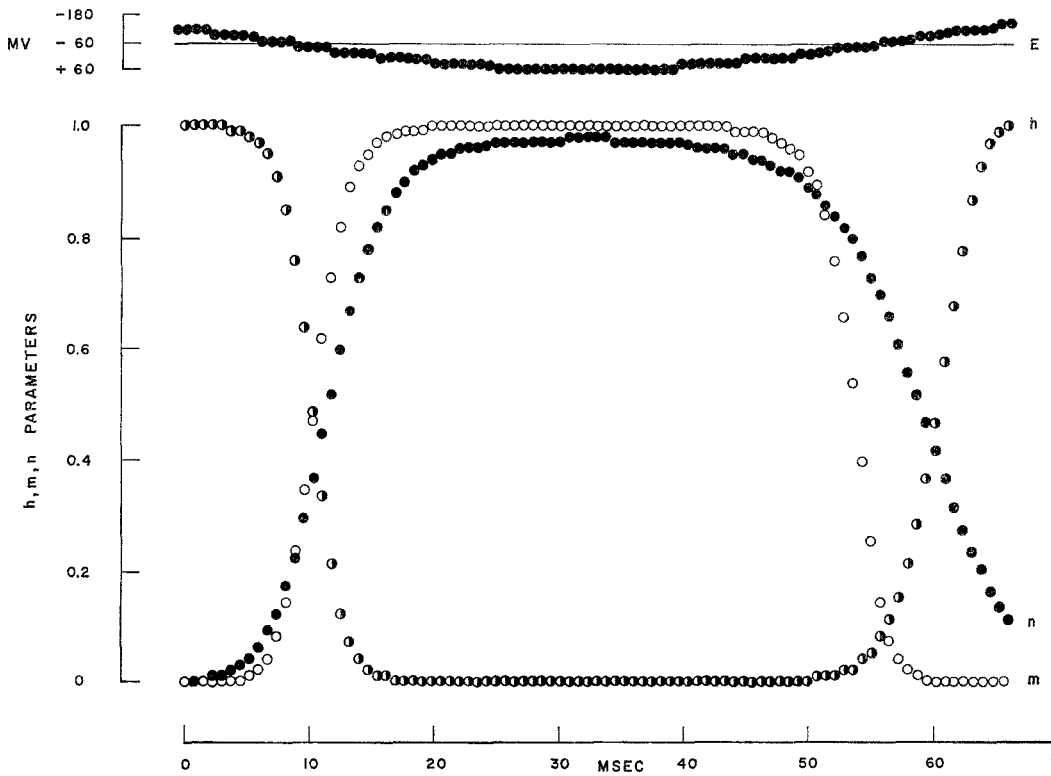

Fig. 4. Computer readout of Hodgkin-Huxley m, n and h parameters plotted as a function of time during a sine wave voltage clamp of $f=10$ Hz and amplitude of ± 120 mV, symmetric with respect to $E_H=-60$ mV. Ordinate: upper trace, E_m change from just before beginning of depolarization. Downward inflection depolarization. Lower trace, m, n and h values: minimal value is 0.0, maximal value is 1.0. Abscissa: time in msec. Note initial saturation of h at maximal value of 1.0 and initial saturation of both m and n at minimal values of 0.0. At peak of depolarization, h is at zero while n is close to maximal. Other details as in Fig. 3

onset of depolarization, an initial small inward current, carried mostly by Na^+, appears and rapidly gives way to a long outward current which lasts throughout the depolarizing phase. Almost from the beginning, this outward current is practically pure (98 to 99%) potassium current. This finding is due to the following: (1) at this low frequency, I_C is negligible ($I_C=C_m \cdot dE_m/dt$); (2) after a brief initial delay, I_{Na} is rapidly turned off by the sodium inactivation (the rate of change of which can follow this slow frequency); and (3) $I_K \gg I_L$ for the voltages considered. Therefore, the membrane currents generated under these conditions reflect the membrane potassium I-V characteristics over a range of 120 mV. Corresponding computed I-V relationships are presented in Fig. 6A. Both potassium

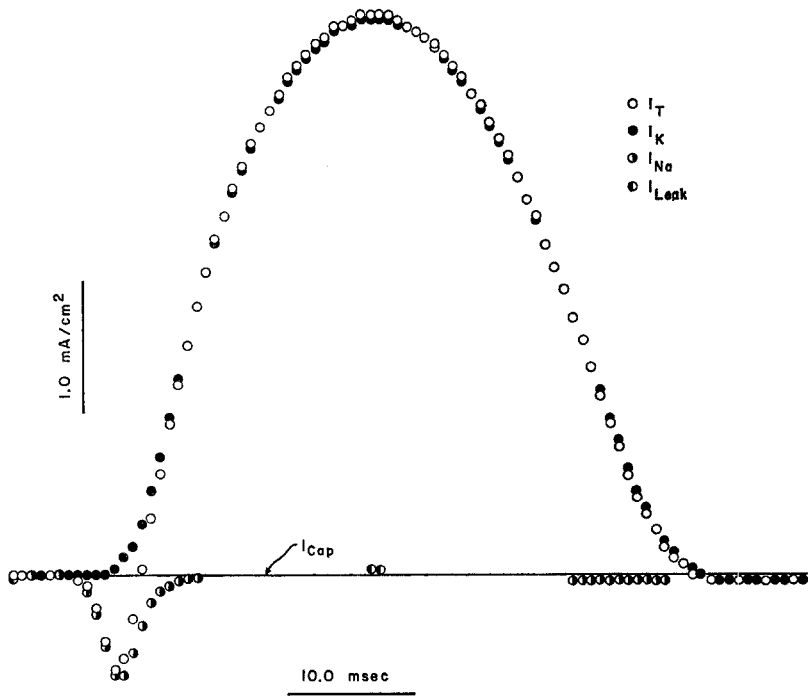

Fig. 5. Computer readout of membrane currents generated by an axon voltage clamped to a 10 Hz, ± 120 mv sine wave (corresponding to the E_m and parameter changes plotted in Fig. 4). Ordinate: membrane currents. Maximal $I_{Na} = -809.3$ μA/cm², maximal $I_K = 4.297$ μA/cm². Outward current plotted upward. Abscissa: time in msec. Calibration of ordinate and abscissa given by bars on figure. Other details as in Fig. 2. Note almost complete current rectification and negligible difference between I_T and I_K

(continuous trace) and sodium (interrupted trace) currents are negligible during the hyperpolarizing half-cycles. At the onset of depolarization (the assumed resting potential of the nerve serving as a model for computation was -60 mV), there is first an inward sodium current (compare with Fig. 5). However, this current is soon inactivated so that upon depolarization of the nerve beyond $E_m = +5$ mV, and upon repolarization of the nerve from $E_m = +60$ mV up to and beyond -80 mV, $I_{Na} = 0$. Since $I_C \simeq 0$ and $I_K \gg I_L$ at this low frequency, the total membrane current equals I_K (the maximal difference between I_K and I_T in this range is 2%), and the membrane I-V relationship is the potassium I-V relationship. Since the potential changes at this low frequency are very slow with respect to τ_n, the potassium I-V relationship of Fig. 6A represents the so-called steady state I-V curve, and, indeed, the shape of the referred part of the I-V curve (with arrow pointing to the left) closely resembles the well-known steady state I-V curves obtained with the step clamp. Such I-V relationships

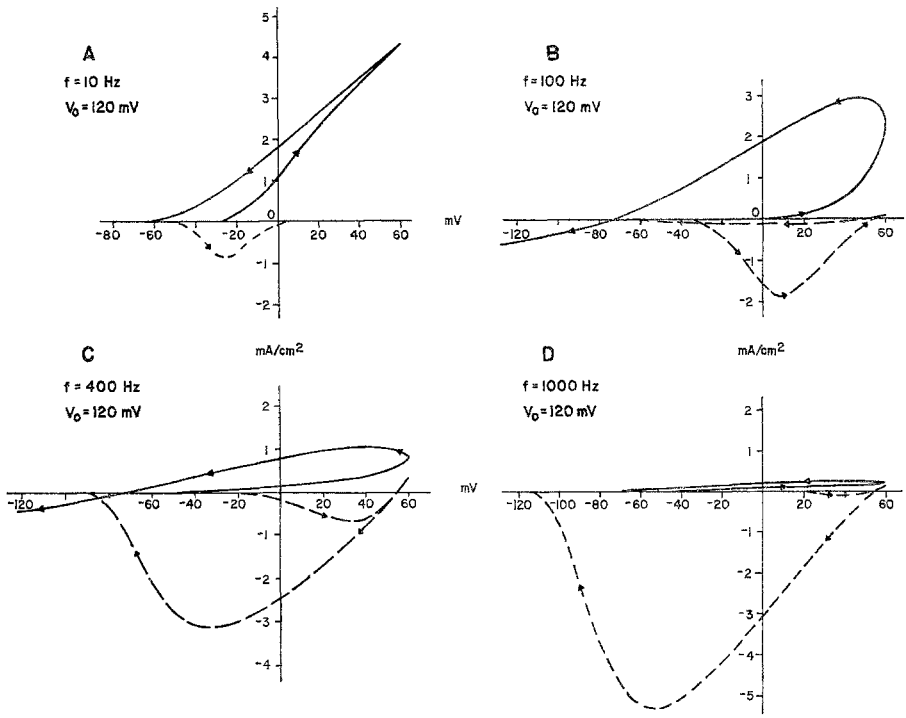

Fig. 6. Computed potassium (continuous line) and sodium (interrupted line) current-voltage characteristics of an axon voltage clamped to sine waves of four different frequencies: 10 Hz in A, 100 Hz in B, 400 Hz in C, and 1,000 Hz in D. Wave amplitude was ± 120 mV, symmetric with respect to the holding potential E_H of -60 mV. Arrows indicate direction of potential and current changes. Ordinate: membrane currents in mA/cm^2, outward current up. Abscissa: membrane potential, E_m, in mV. Note predominance of I_K at 10 Hz and I_{Na} at 1,000 Hz. Further details in text

obtained by means of a sine or triangular wave can be directly displayed on the oscilloscope screen by connecting the membrane potential (as measured during voltage clamp) to the X input and the membrane current to the Y input of an oscilloscope.[4]

Fig. 7 plots the computed membrane currents as a function of time for an intermediate frequency (100 Hz) and moderate amplitude ($E_m = \pm 50$ mV) sine wave. At this frequency, the degree of turn-on of the potassium conductance parameter, n, is relatively small. Capacity current at this frequency is still negligible so that the major component is I_{Na} throughout most of the depolarizing phase. Increasing the wave amplitude to ± 120 mV, as illustrated by means of the appropriate I-V relationship in Fig. 6B, results in

[4] Note that upon applying both the triangular and the sine voltage waves to the horizontal amplifier of the oscilloscope, the x axis becomes a linear function of voltage.

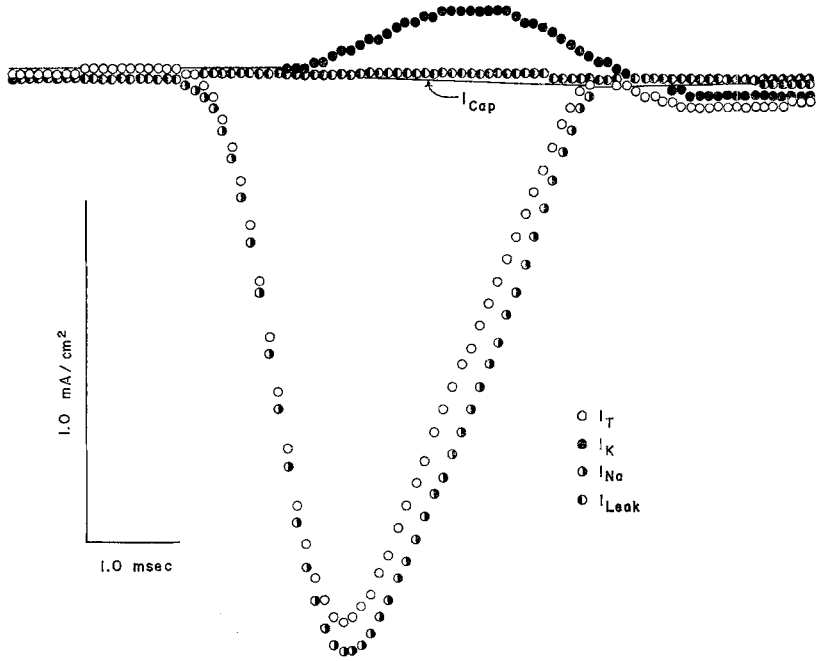

Fig. 7. Computer readout of membrane currents generated by an axon voltage clamped to a 100 Hz, ±50 mV sine wave. Ordinate: membrane currents. Inward current plotted downward. Maximal $I_{Na} = -1.7091$ mA/cm². Maximal $I_K = 201.9$ μA/cm². Abscissa: time in msec. Note similarity between I_T and I_{Na}. For further details, see text

a higher I_K so that I_m now reflects I_{Na} when the membrane is depolarized and I_K upon repolarization.

Fig. 8 plots the computed m, n and h parameter changes as a function of time for a relatively high frequency (400 Hz) and moderate amplitude ($E_m = \pm 50$ mV) triangular wave. At this frequency, the changes of the slow potassium conductance parameter, n, are very small. Similarly, the decrease in h and, therefore, the increase in the level of sodium inactivation (during depolarization) are small. However, at the same time, the sodium activation parameter, m, increases about 10-fold. During the depolarization phase of such a cycle, the main component of I_m is therefore I_{Na}, as illustrated in Fig. 9 (compare also with Fig. 6C derived for a similar sine wave). In the frequency and amplitude ranges mentioned above, one obtains I_m values (I_T) which reflect the I_{Na} values with an accuracy of about 95%. At higher frequencies, I_K is reduced further. Fig. 6D illustrates the Na^+ and K^+ I-V relationship for $f = 1{,}000$ Hz and $E_m = \pm 120$ mV. I_K is seen to be negligible with respect to I_{Na}. I_{Na} gives a typical peak sodium current-voltage relationship with a negative conductance zone. At this frequency, I_C cannot be ignored. However, as described below, one can easily correct

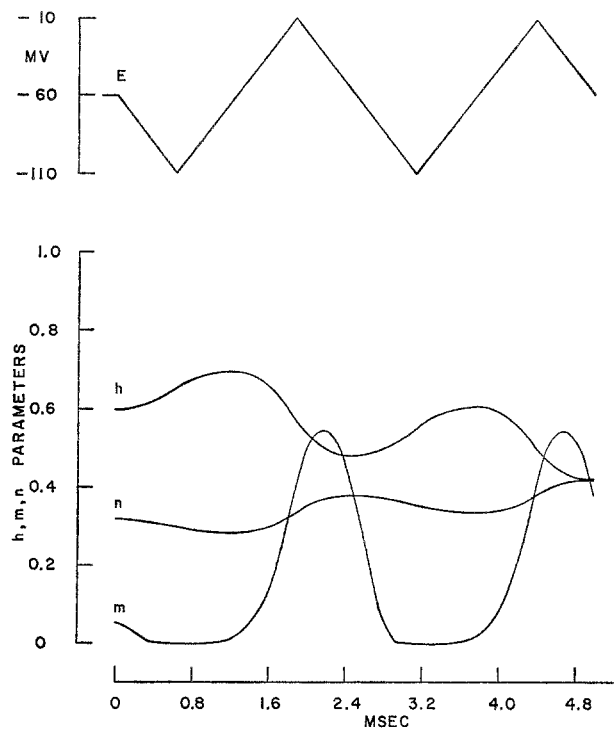

Fig. 8. Computer readout of Hodgkin and Huxley m, n and h parameters plotted as a function of time during a triangular wave of $f=400$ Hz and amplitude of ± 50 mV. Ordinate: upper trace, membrane potential changes in mV. Lower trace, m, n and h values. Abscissa: time in msec. Other details as in Fig. 3

I_m for I_C since the values of I_C at any time can be easily determined for both triangular waves (when I_C is a square wave) and sine waves (when I_C is a cosine wave).

The leakage current, I_L, can be studied by means of a sine or linearly varying potential clamp using hyperpolarizing potentials, i.e., when I_{Na} and I_K become negligible. Fig. 10 illustrates the computed membrane currents for a triangular wave of $f=20$ Hz and E_m increasing from resting level of -60 mV to -180 mV. When E_m returns from -180 mV to resting level, the maximal values of I_{Na} and I_K are less than 0.1 $\mu A/cm^2$ so that $I_{Na} \ll I_L \gg I_K$. From the slope of I_m in Fig. 10, one can therefore obtain both g_L and I_L as a function of E_m. Any experimental deviation of the upward stroke of I_m from linearity would indicate leakage current rectification.

If the varying potential is of a proper amplitude, at some instant it must equal the reversal potential of any ionic current. If one chooses conditions such that I_T equals the ionic current in question, the potential

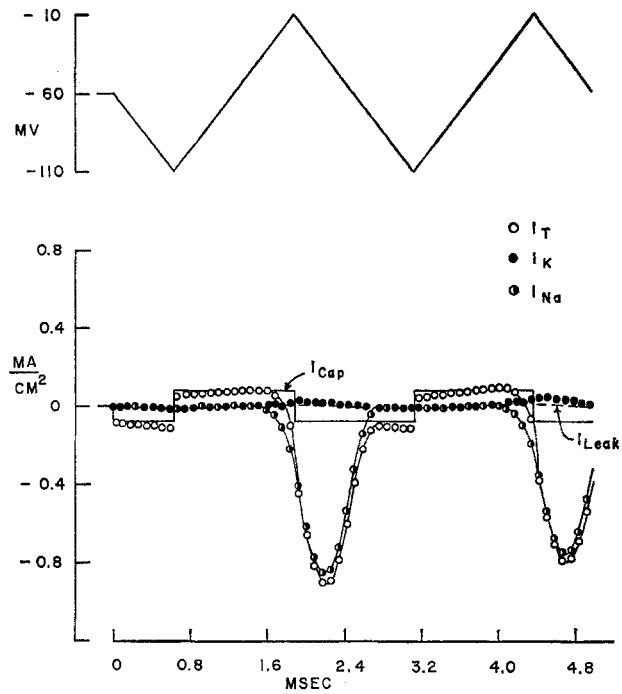

Fig. 9. Computer readout of membrane currents generated by an axon voltage clamped to a 400 Hz, ± 50 mV triangular wave (the corresponding m, n and h changes are given in Fig. 8). Ordinate: upper trace, membrane potential changes. Lower traces, membrane currents. Inward currents plotted downward. Abscissa: time in msec. Note similarity between I_T and I_{Na} changes. For further details, see text

corresponding to the $I_T = 0$ point is the reversal potential of the ion. For example, the reversal potential of I_K, E_K, can be determined by means of this procedure from the point where I_T crosses the zero line at the end of the depolarizing phase in Fig. 12H. In the determination of E_K using a wave of $f = 21$ Hz and $E_m = \pm 120$ mV, or in the determination of E_{Na} using a wave of $f = 1{,}000$ Hz and $E_m = \pm 150$ mV, the computed error is less than 1 mV.

When a potential wave generating a membrane current which equals I_{Na} or I_K is suddenly terminated, the specific current decays with its typical time constant from which τ_m and τ_n can be determined.

As can be seen in Fig. 12C and G (*see* also Fig. 3), the first few cycles may differ from the following ones when relatively high frequencies are used. However, in all cases investigated, the response reached a steady state within a few cycles. This transient is due to the fact that one or more of the time constants of the conductance parameters (τ_m, τ_n, τ_h) are slow with respect to the frequency (*see* description of Fig. 3 above). This transient

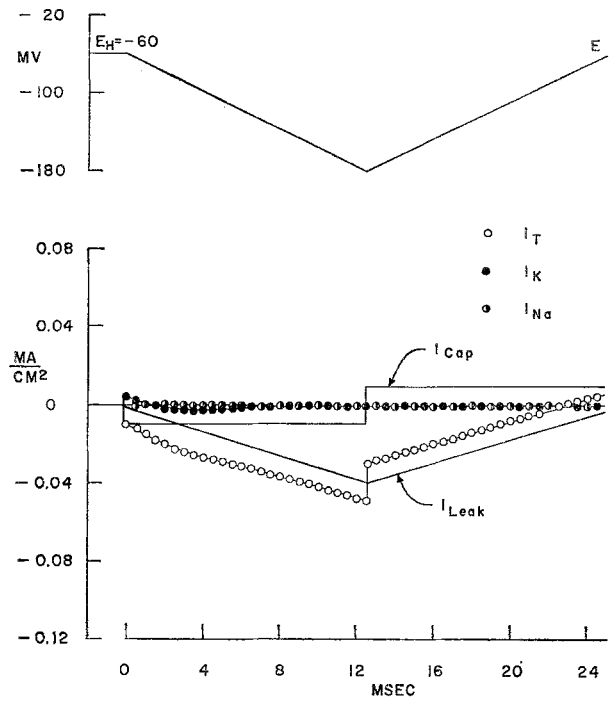

Fig. 10. Computer readout of membrane currents generated by an axon voltage clamped to a membrane potential linearly changed from $E_H = -60$ mV to -180 mV and then linearly back to -60 mV. Duration of each slope is 12.5 msec. Ordinate: membrane currents. Abscissa: time in msec. Note that the slope of I_T equals that of I_{Leak}. Further details in text

does not interfere with utilization of the first or any of the subsequent cycles for current separation.

Membrane Capacity. Membrane capacity current, I_C, is given by:

$$I_C = C_m \, dv/dt. \tag{15}$$

For a linearly varying potential, dv/dt is a constant for each slope. Therefore, the capacity current generated by a membrane voltage clamped to a triangular wave would be a square wave. The current associated with a sine wave would be a cosine wave. As seen in Fig. 12F, high frequency-low amplitude sinusoidal potential waves generate cosine capacitive current waves. However, it is difficult to detect any small non-capacitive current components on top of this type of wave. Measurement of C_m by sine waves may, therefore, be carried out accurately only under conditions where the ionic currents are known to be negligible. Interesting information can, however, be obtained from the phase shifts associated with such sine waves.

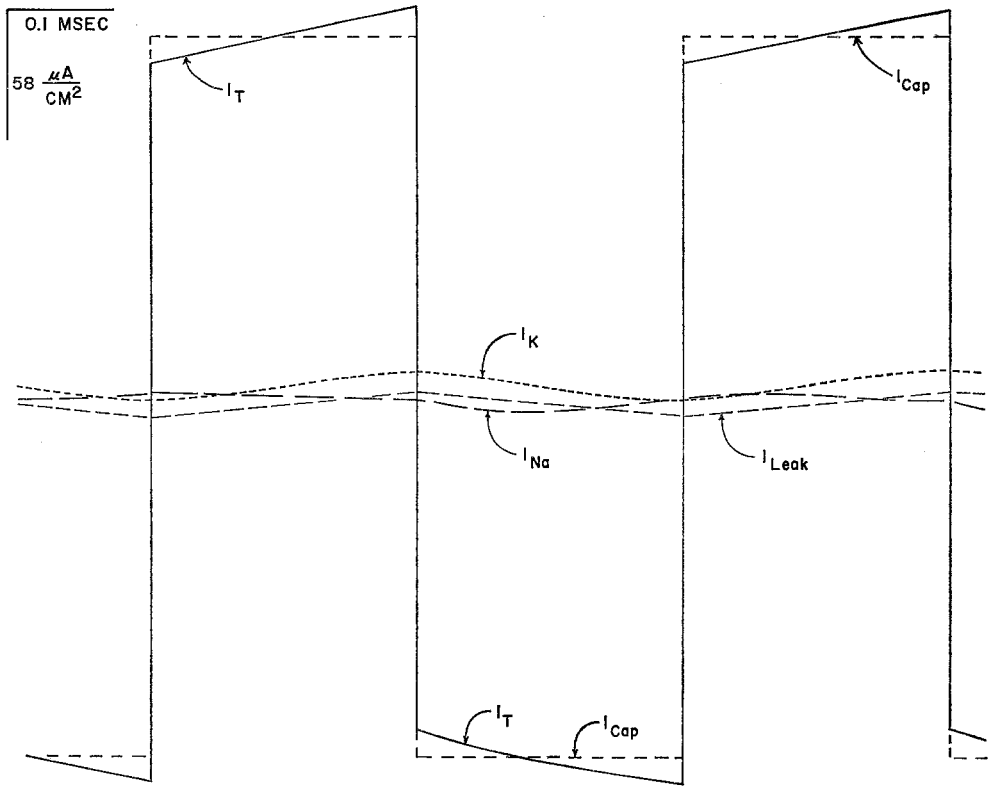

Fig. 11. Computer readout of membrane currents generated by an axon voltage clamped to a triangular wave of 2,000 Hz and amplitude of ± 10 mV, symmetrical with respect to the holding potential, $E_H = -60$ mV. Ordinate: membrane currents. Maximal $I_{Cap} = \pm 160$ μA/cm². Abscissa: time in msec. Note that the jumps in I_T equal those of I_{Cap}

As illustrated in Fig. 11, the membrane current generated by a triangular wave of relatively high frequency (2,000 Hz) and low amplitude ($E_m = \pm 10$ mV) is mostly capacitive. The jump of I_T associated with the change of the slope of E_m is seen to be equal to the jump in I_C. From this jump, membrane capacity, C_m, can be easily determined in microfarads from:

$$C_m = \frac{I_0 \lambda}{4 V_0} \tag{16}$$

where I_0 and V_0 are the peak-to-peak amplitude of the square and triangular waves in μA and mV, respectively, and λ is the wavelength in msec. Any unexpectedly large ionic current which may introduce an error into C_m determination can easily be detected, as it would result in a distortion of the square I_m wave. The accuracy of this method can be increased

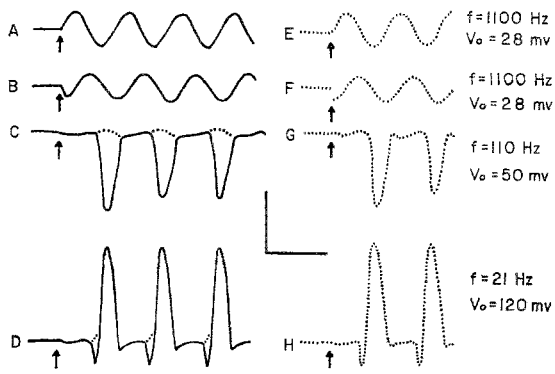

Fig. 12. Typical experimental and calculated current and voltage traces of axons voltage clamped to sinusoidally varying potentials. V_0 is the holding potential to peak amplitudes. Holding potential was at resting potential in the living axon and -60 for the computed model axon. *A*, an experimental E_m trace from an axon voltage clamped to a sine wave of 1,100 Hz and ± 28 mV. *B*, the experimental trace of I_m obtained upon clamping an axon to the varying E_m illustrated in Fig. 12A. *C* and *D*, the experimental traces of I_m obtained upon clamping axons to sine waves of 110 and 21 Hz, respectively. In *C*, $V_0 = 50$ mV and in *D*, $V_0 = 120$ mV. Interrupted line is I_m trace obtained in ASW in which all Na^+ was substituted by $Tris^+$. *E* values of E_m calculated for the same conditions as the experimental trace of Fig. 12A. *F*, *G*, *H* values of I_m calculated for the same conditions as the experimental traces of Fig. 12*B*, *C* and *D*, respectively. Arrows indicate beginning of sine oscillation. Horizontal bar = 1 msec in *A*, *B*, *E* and *F*, 10 msec in *C* and *G*, and 50 msec in *D* and *H*. Vertical bar = 100 mV in *A* and *E*, 1 mA/cm^2 in *B*, *C*, *F* and *G*, and 2 mA/cm^2 in *D* and *H*. For further details, see text

to better than 1% in the 1 kHz range by averaging the currents generated by consecutive potential waves. In this connection, one should note that: (1) in living cells, capacity measurements by means of AC bridges involve very complex instrumentation and techniques which make this method unsuitable for routine use; and (2) membrane capacity determination by means of the transient associated with a step potential change, as carried out by Hodgkin and Huxley (1952) for example, depends on very accurate measurement of the time course of a transient lasting about 10 μsec. The accuracy of the determination is further reduced as there is no simple and accurate way to correct the measured current for the ionic current component. The actual analysis of the data obtained with this method is considerably more time-consuming than that needed with triangular waves.

Experimental

Membrane Current Measurements. A typical membrane current recorded from an axon voltage clamped to the low-amplitude (± 28 mV), high-frequency (1,100 Hz), sinusoidal potential wave illustrated in Fig. 12A is

Table 1. *Artificial sea water (ASW) solutions*[a]

Solution	Concentration (mM)					
	$[Na^+]$	$[K^+]$	$[Tris^+]$	$[Ca^{++}]$	$[Mg^+]$	$[Cl^-]$
Normal ASW	430	10	0.5	10	50	560
K-free ASW	440	0	0.5	10	50	560
10 mM K, 230 mM Na ASW	230	10	200.0	10	50	560
50 mM K, 230 mM Na ASW	230	50	160.0	10	50	560
100 mM K, 230 mM Na ASW	230	100	110.0	10	50	560
210 mM K, 230 mM Na ASW	230	210	0.5	10	50	560
Tris ASW (Na-free)	0	10	430.0	10	50	560
Ca ASW (Na-free)	0	10	0.5	297	50	704
Ca-, Mg-free ASW	490	10	0.5	0	0	500

[a] In all solutions, pH = 7.4.

given in Fig. 12B. The locus of I_m in time is a sine function shifted by 90° with respect to E_m. Currents practically identical to those illustrated in Fig. 12B were obtained when a similar experiment was carried out in ASW, in which all sodium chloride (430 mM) was replaced by Tris Cl (*see* Table 1). Therefore, little, if any, of this current is carried by sodium ions. Since the values of I_K and I_L are negligible under these conditions (*see* Analytical section), the computed I_C values are seen in Fig. 12F to be identical with the experimental I_m curve. Therefore, it may be concluded that the experimental I_m curve is capacitative.

The well-behaved sine-like currents generated under the above conditions give way to more complex forms at lower frequencies.

Fig. 12C gives I_m as a function of time for a sine wave of ± 50 mV and 110 Hz. A large inward current is generated in the depolarizing phase (continuous trace). The calculated values of I_m (Figs. 7 & 12G) agree very well with this experimental trace. When all the Na^+ is replaced by $Tris^+$ in the ASW, the inward current is completely abolished (interrupted line of Fig. 12C). The inward current measured in normal ASW is, therefore, carried by sodium ions. Potassium currents remain negligible as the duration of the depolarizing phase is short relative to the rate of turn-on of I_K. Thus, under the above experimental conditions, one can obtain a sodium I-V relationship "on line" by feeding I_m to the horizontal plates and E_m to the vertical plates of an oscilloscope.

A typical I_m trace obtained in ASW from an axon voltage clamped to sine waves of 21 Hz and ± 120 mV is given in Fig. 12D. The membrane current generated upon depolarization is mostly outward. The experimental

current trace is seen again to be in excellent agreement with the computed values (Fig. 12H; *see* also Figs. 5 & 6A). At such a low frequency, I_{Na} does not reach an appreciable value because of the development of sodium inactivation (*see* Analytical section). Substitution of all of the Na^+ in the ASW by $Tris^+$ only results in abolition of the initial transient inward current (interrupted line, Fig. 12D). Since I_C is negligible at this low frequency and since $I_K \gg I_L$, the current in Fig. 12D represents I_K during most of the cycle. As explained in the previous section (Analytical), the rate of change of potential at 20 Hz and below is slow when compared with the rate of change of I_K. Therefore, I_m in Fig. 12D can be regarded as a good approximation of the so-called steady state I_K (*see* Fig. 6A).

Typical examples of sodium and potassium I-V relationships at a low and at a high frequency are illustrated in Fig. 13. Both at low frequencies where potassium currents predominate (Fig. 13A) and at high frequencies where sodium currents predominate (Fig. 13B), we see that the experimental curves are in good agreement with the I-V curves calculated for the same conditions. Whereas the potassium I-V curve is very similar to the steady state or potassium I-V curve obtained by means of the step clamp, the sodium curve is somewhat different. However, except for extreme hyperpolarizations, the sodium curve can serve just as well for characterization of the sodium I-V relationship as the one derived from step clamp data.

The reversal potentials for sodium and potassium have been determined from the point where the membrane current (which under the appropriate conditions equals the specific current in question) crosses the zero axis, as explained in the previous section. The waves used for such determinations were of 10 to 20 Hz, $E_m = \pm 120$ mV for E_k, and of 100 to 200 Hz, $E_m = \pm 150$ mV for E_{Na}. The values of reversal potential thus obtained were within ± 1 mV of those obtained in the conventional manner (Hodgkin & Huxley, 1952*a*, *b*), by means of the standard step clamp. The values of E_k and E_{Na} were also determined when $[K_0]$ and $[Na_0]$ were changed. The values determined under these conditions were also in agreement with the computed E_k and E_{Na} values. As one can determine the zero crossover point with ease and great accuracy, the E_{Rev} values obtained by the sine clamp can be considered reliable. In case of high noise levels, average values from consecutive cycles can be utilized to increase accuracy.

Fig. 14 illustrates the effect of high external $[K^+]$ (210 mM) on inward sodium current. When ASW is replaced by Na-free Tris ASW, the main component of the inward current (carried by Na^+), disappears. Exactly the same reduction in I_m is obtained upon replacing half of $[Na_0]$ by 210 mM $[K_0]$. One may therefore conclude that high $[K_0]$ completely

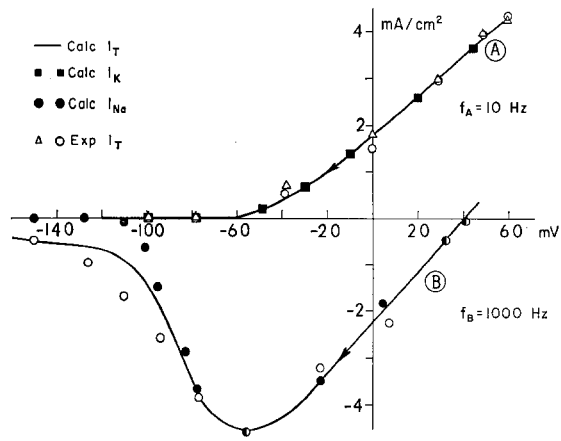

Fig. 13. Typical experimental and computed membrane currents of an axon voltage clamped to a sinusoidally varying potential as a function of membrane potential (I-V curves). $E_H = -60$ mV. Frequency is 10 Hz in *A* and 10^3 Hz in *B*. *A*, continuous line, computed I_m values. Solid squares are computed I_K values. Open circles and triangles are experimental values from two nerves. *B*, continuous line represents computed I_m values. Solid circles are computed I_{Na} values. Open circles are experimental values. For further details, see text

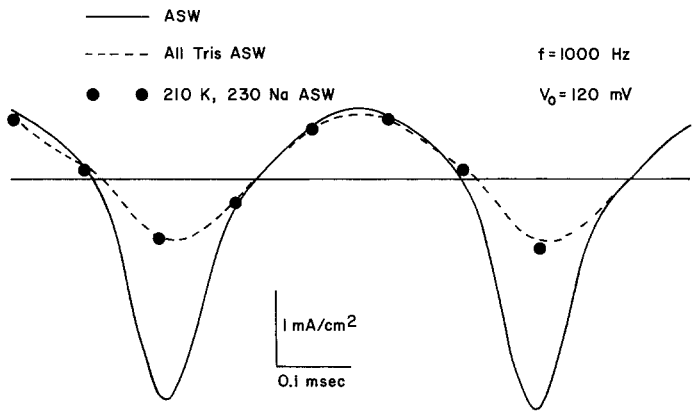

Fig. 14. The effect of high $[K_0]$ (210 mM) on inward sodium current in an axon voltage clamped to a sine wave of $f = 1{,}000$ Hz and amplitude of ± 120 mV, symmetrical with respect to the original resting potential of the nerve in ASW, -59 mV (the resting potential in 210 mM K ASW was -24 mV). The axon membrane potential was held for at least 2 sec at -59 mV before the sine wave was applied. Continuous trace: I_m in ASW. Interrupted trace: I_m in Na-free ASW. Solid points: values of I_m in 210 mM K, 230 mM Na ASW. Note identical attenuation of inward current in Na-free and 210 mM K ASW. Further details in text

abolishes the inward sodium current throughout the 120 mV depolarizing potential range. This result is in agreement with the sodium-potassium interactions described for lower $[K_0]$ and more limited potential range by Adelman and Palti (1969).

Membrane Capacity Measurements. Figs. 15 and 16 illustrate the membrane currents generated by triangular potential waves under the conditions where the total ionic current is small with respect to I_C (*see* Analytical section). In Fig. 15, the total current is, as expected, a square wave with negligible ionic components. Eq. (16) was used to compute the membrane capacity, C_m, from such data for 10 axons, over the frequency range of 100 to 2,000 Hz and peak-to-peak potential variations in the range of 10 to 300 mV. Numerous measurements were carried out in each axon, and in each measurement the amplitudes of a few consecutive waves were

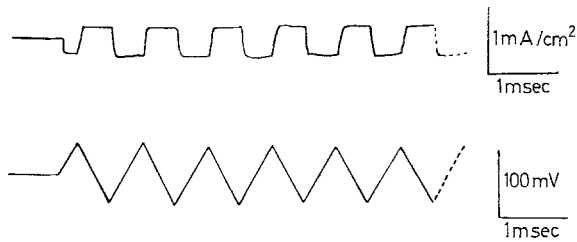

Fig. 15. Typical capacity current wave (upper trace) generated by an axon voltage clamped to a triangular potential wave (lower trace) of $f=900$ Hz and amplitude of ± 40 mV. Note the square wave shape of the membrane current

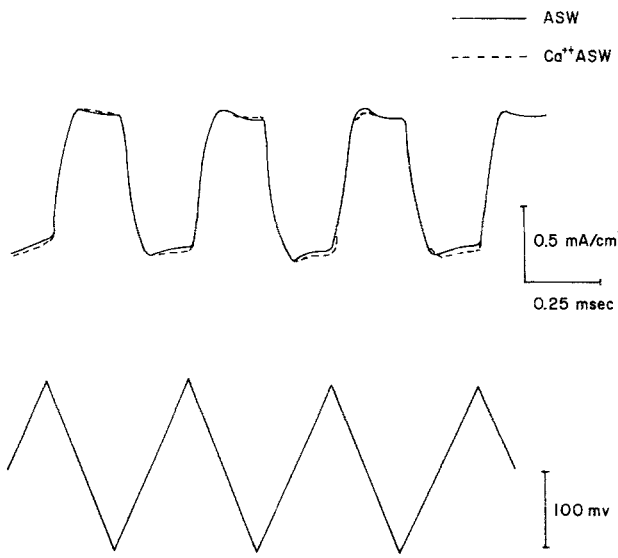

Fig. 16. The effect of replacing all the Na^+ by isosmotic amounts of Ca^{++} (*see* Table 1) on membrane capacity. Upper trace: membrane currents generated by an axon voltage clamped to the triangular potential wave of $f=1{,}800$ Hz and amplitude of ± 100 mV given in the lower trace. Note negligible change in the amplitude of the square wave which indicates no C_m changes

Table 2. *C_m values in ASW solutions*

Solution	Frequency (Hz)	Average C_m ($\mu F/cm^2$)	Standard deviation	No. of measurements[a]	C_m values ($\mu F/cm^2$) min.	max.
ASW	2,000	1.07	0.10	44	0.93	1.39
ASW	1,000	1.09	0.10	60	0.93	1.39
ASW	500	1.12	0.14	38	0.85	1.67
ASW	200	1.07	0.15	32	0.70	1.41
ASW	100	1.30	0.49	21	0.85	2.50
K-free ASW	1,000	1.02	—	2	1.02	1.02
50 mM K, 230 mM Na ASW	1,000	1.02	0.09	7	0.93	1.18
100 mM K, 230 mM Na ASW	1,000	1.06	—	2	1.04	1.08
210 mM K, 230 mM Na ASW[b]	1,000	1.15	0.12	6	1.03	1.32
10 mM K, 230 mM Na ASW	1,000	1.02	0.17	8	0.96	1.10
Tris ASW (Na-free)	1,000	1.07	0.08	18	0.95	1.25

[a] The number refers to the number of records analyzed. The amplitude of two to four consecutive waves in each record was averaged and considered one measurement in the final averaging and standard deviation determination.

[b] Measurement was made when E_m was held for at least 3 sec prior to the C_m measurement (by means of a voltage clamp) at the value of E_m obtained in normal ASW.

averaged.[5] The average membrane capacity thus obtained was 1.09 $\mu F/cm^2$ ± 0.1 SD at 1 kHz. As can be seen in Table 2, the variations of C_m in the 200 to 2,000 Hz frequency range are negligible.[6] Below 200 Hz, the average C_m value increases considerably above the typical 1 μF value. However, as I_C becomes very small in this range, the accuracy of the measurement is much lower. The capacitive current retained its square wave shape, even when the triangular wave amplitude was over 200 mV, indicating a negligible voltage dependency of C_m.

A similar set of capacity measurements was carried out when the external ASW was replaced by a variety of solutions. A typical example of such a measurement from an axon externally perfused with Ca ASW (*see* Table 1) is given in Fig. 16. The change in I_C and thus C_m, if any, is negligible (*see* also Table 2). Similar results (i.e., very small and probably insignificant C_m changes) were obtained in Na-free ASW (Tris is assumed to be nonpermeable through the axon membrane), Ca- and Mg-free ASW, and 230 mM Na ASW with [K] ranging from 10 to 210 mM (*see*

[5] The number of measurements indicated in Table 2 refers to the number of records analyzed. The amplitude of two to four consecutive waves in each record was averaged and considered one measurement in the final averaging and SD determination.

[6] Note that for a 2 kHz triangular wave, the frequency components above 10 kHz are negligible.

Table 3. *Average C_m values in ASW solutions*

Solution	Frequency (Hz)	Average C_m ($\mu F/cm^2$)
ASW	1,000	1.07[a]
Ca-, Mg-free ASW	1,000	1.25
ASW	2,000	1.11[a]
Ca-, Mg-free ASW	2,000	1.19
ASW	1,000	1.11[a]
Ca ASW (Na-free)	1,000	1.05
ASW	2,000	0.97[a]
Ca ASW (Na-free)	2,000	0.95

[a] Average of values of C_m obtained in ASW before and after the specific solution change.

Tables 2+3). In 210 mM K, 230 mM Na ASW, when E_m dropped below -20 mV, the leakage current increased over 10-fold and C_m was increased by an average of 50%. This increase was reversed upon returning to ASW or when E_m was held at normal resting values by means of the voltage clamp. Axons in isosmotic dextrose (0.834 M), with 10 to 50 mM Tris added to maintain the conductivity of the medium, showed about a 30% increase in C_m.

Effect of Temperature on Membrane Capacity. The temperature dependency of C_m is illustrated in Fig. 17. From 3 to 22 °C, C_m has a positive temperature coefficient. The average change is 1.36%/°C. In this temperature range, the C_m change is completely reversible. Elevating the temperature further to 40 °C fails to show any significant change in C_m. If one chooses to ignore the change of slope of the curve at about 20 °C and to calculate the slope for the entire 3 to 40 °C range, an average slope of 0.93%/°C is obtained. Above 40 °C, the C_m vs. °C curve breaks so that C_m increases greatly with temperature and reaches values of over three, close to 50 °C. The slope at this range is at least 23%/°C. At about the same temperature that the slope of the C_m vs. temperature curve begins to increase sharply, the leakage current, I_L, increases. I_L, which is practically undetectable (g_L below 1 mmho/cm^2) up to 33 °C, begins to show a slow increase above this temperature. However, only at about 42 °C (when $g_L \simeq 10$ mmho/cm^2) does I_L begin to increase sharply with temperature reaching a value of 200 mmho at 49 °C. In the 44 to 49 °C range, g_L increases 20-fold. In the above experiments, the nerve membrane potential is only slightly affected by the increase in temperature up to 30 °C. From 30 to 39 °C, E_m decreases by 13 mV (note that in this range C_m is constant), and from 39 to 44 °C

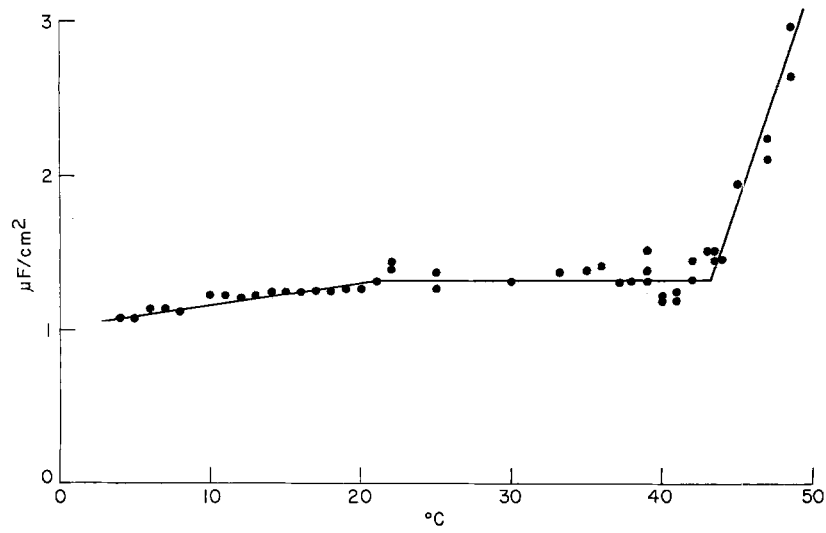

Fig. 17. Temperature dependency of membrane capacity. Ordinate: values of membrane capacity calculated by means of Eq. (16) from I_m values, measured from an axon voltage clamped to a triangular wave of $f=1{,}000$ Hz. Abscissa: temperature of the solution surrounding the axon in the voltage clamping chamber. The temperature was increased from 3 °C at a steady rate of about 1/2 a degree per minute. The slope of the curve between 3 and 21 °C is 1.36 %/°C. The slope of the curve beyond 42 °C is at least 23 %/°C

by an additional 20 mV. Beyond this temperature, E_m decreases only slightly as temperature increases. The above changes in C_m and I_L in the temperature range where E_m decreases were observed when E_m was held at the original resting level for at least 3 sec prior to the measurements. Above 39 °C, the changes in C_m and I_L with temperature became considerably larger when measurements were taken from the depolarized membrane. It seems likely that I_C and I_L are parallel functions of temperature, but are not dependent on each other.

Discussion

Analysis of the behavior of an axon membrane clamped to a varying potential predicts that by choosing the proper frequencies and amplitudes, one may: (1) separate the total membrane current, I_m, into its components (I_{Na}, I_K, I_L and I_C); (2) obtain direct "on line" display of the total and separated ionic I-V characteristics; (3) obtain accurate determinations of E_{Na} and E_K; and (4) determine membrane capacity with ease and a high degree of accuracy. The accuracy of current separation and ease of obtaining direct I-V relationships is roughly the same for the sine and triangular

waves. Sine waves have a slight advantage in obtaining pure potassium currents at low frequencies, whereas linearly varying currents are more efficient for the separation of I_{Na} from I_C at relatively high frequencies and also yield more accurate I_C or C_m determinations. The above predictions, based on the Hodgkin-Huxley axon model, were found to be in good agreement with the experimental results. The requirements, in terms of frequency-response bandwidth, of the electronic systems for the sine-mode voltage clamp are much lower (up to about 5,000 Hz) than those of the step clamp (up to 10^6 Hz) or even the linearly varying potential mode. This fact may make it possible to voltage clamp membranes which, because of their extremely high electrode impedances, etc., cannot be clamped by the step clamp method.

In such cases, the interpretation of the results does not depend on analytical data obtained by means of a step clamp. It is only made easier when such information is available, as is the case with the giant axon of the squid. In the case of a new preparation which behaves significantly differently from the squid, whether one uses a step or a varying potential clamp one has to conduct new analyses, current separations by chemical substitutions, etc. However, such an analysis is possible for both modes of voltage clamp. The analysis may be easier when using the step clamp when the different ionic current components have very similar kinetics and computer aid is not readily available.

The study of preparations which produce very small membrane currents and involve low signal-to-noise ratios may also be aided by an oscillating clamp since the currents produced by consecutive cycles can be readily averaged. However, when noise levels are low, which is the case for many preparations, all the useful information can be obtained from a single cycle, i.e., within a few milliseconds which is ideal for kinetic studies.

In contrast to the data obtained by the standard clamp, or even the triangular wave or ramp clamp, the data obtained with a sine wave voltage clamp are compatible in form with the available forms of physical and physico-chemical parameters (e.g., dielectric constants). The sine clamp data can be readily utilized for construction and analysis of electric analog systems consisting of resistive, capacitive, and inductive elements, as well as of solid-state elements.

The varying potential clamping mode does not usually offer any advantage over the step clamp for the determination of the conductance time constants. Although τ_n and τ_m can be determined by terminating the wave (in analogy to such determinations from tail current decay when using the step clamp), no simple way to determine τ_h has been found.

The values of membrane capacity found in this work at 1 kHz using the voltage clamp are not significantly different from those originally reported by Curtis and Cole (1938) [1.3 $\mu F/cm^2$] or more recent works carried out using the bridge method. However, the frequency independence of C_m in the 200 to 2,000 Hz range stands in contrast to many reports on C_m variations with frequency in this range, i.e., the α dispersion (Cole, 1968). However, these C_m determinations were done by means of external electrodes, whereas those reported here were made across the cell membrane. Taylor and Chandler's (1962) and Taylor's (1965) determinations were the only ones which were carried out by means of internal and external electrodes, and which did not extend below 10 kHz. Therefore, it seems likely that the so-called α dispersion of the membrane dielectric constant, ε, found in the low-frequency range by investigators using external electrodes is due to a surface admittance relaxation caused by counter-ion movement (Schwan, 1965). The independence of C_m from frequency found in this work is in agreement with the dielectric behavior of artificial bilayer lipid membranes (Hanai, Haydon & Taylor, 1965).

The temperature dependency of membrane capacity found in this work is in general agreement with that reported by Taylor (1965) for the 5 to 21 °C range at 10 kHz. The positive temperature coefficient of C_m can be attributed to an increase in membrane dielectric constant with temperature or to a thinning of the membrane under these conditions. The thickness change predicted on the basis of the C_m changes in the 3 to 21 °C range is about 25%. Such a dimensional change, which is not accompanied by a significant change in membrane selectivity properties, does not seem probable, although it may be possible. A gradual increase with temperature in the dielectric constant, which eventually reaches a plateau, is generally unexpected from dielectric behavior in static fields. However, such a change can be expected in dynamic fields from the following considerations of dielectrics.

Let us consider first, for simplicity, that the polarizibility of the membrane is determined by asymmetry of distribution of an ion species between two stable sites, A and B, separated by an energy barrier, ϕ. Let us consider the case in which the energies of the ions in sites A and B are equal. The probability per second, P_0, of a charged particle jumping from site A to site B is given according to statistical mechanics (Decker, 1959) by:

$$P_0 = \nu \exp(-\phi/KT) \tag{17}$$

where ν is a frequency factor on the order of 10^{12}/sec. Thus on the average, in the absence of an external field, charged particles will be distributed

such that there are $N/2$ ions in A sites and $N/2$ in B sites per unit volume (in our specific case, unit membrane surface), where N is the total number of such ions per unit volume. Let an electric field, E, be applied across the membrane. The field will change the energies in A and B such that charged particles in A sites have to pass a barrier $(\phi - eaE)$ to jump to B, while the barrier from B to A is $(\phi + eaE)$, where e is the electron charge and $2a$ is the distance of separation of sites A from sites B. Under these conditions, ions will prefer B sites over A sites, and an average charge separation or polarization will result. Assuming that for a living membrane (where the jumps are probably in the form of dipole movements) "a" is on the order of a single angstrom, then under normal conditions $eaE < kT$ so that the dipole moment per unit volume or area would be (Decker, 1959):

$$P_{(t)} = \frac{Ne^2a^2E}{2kT}[1 - \exp(-t/\tau)] \tag{18}$$

where:

$$\tau = 1/2P_0 . \tag{19}$$

Note that the first term on the right-hand side of Eq. (18) indicates an inverse relation between P (and, therefore, the dielectric constant, ε) and the temperature T, whereas the second term together with Eq. (19) gives a direct relationship. If we assume for a living membrane that ϕ is on the order of 1 kcal and that the behavior of the membrane dipoles is not significantly different from that of the above charged-particle model, we can compute the relaxation time, τ, by means of the above equations. The computed values of τ are on the order of 10^{-3} sec (i.e., in the frequency range where our experiments were carried out). Under such conditions, the relaxation time decreases with temperature. At a constant frequency (in the above range), polarization and thus the dielectric constant, ε, first increase with temperature and then reach a plateau. Thus, the shape of the first segment of the C_m vs. temperature curve of Fig. 17 can be explained by means of the above model. The break of the curve above 40 °C is most probably due to a phase transition of some component of the membrane, most probably the lipid in the bilayer. For example, such phase transitions in bimolecular egg lecithin leaflets at temperatures of 30 to 40 °C (depending on the amount of hydration) have been described by Small (1967).

The relative independence of C_m of the ionic species in the external medium and even of the ionic strength of the medium may indicate that the major factor responsible for the dielectric behavior of the axon membrane is the membrane matrix itself. Thus, the contribution of the mobile charges distributed as a space charge around membrane fixed charges may

be small. This conclusion stands in contradiction to the hypothesis put forward by Mauro (1962). On the basis of analysis of ion distributions in membranes consisting of regions of fixed charges of opposite signs, Mauro derived the following equation for the capacity (in farads) of such a membrane:

$$C = 1.05(\varepsilon q N / 16\pi \Delta\psi)^{1/2}. \tag{20}$$

In Eq. (20), ε is the dielectric constant of the medium, q is the charge of the mobile particle, N is the fixed charge concentration, and $\Delta\psi$ is the potential difference across the membrane. Eq. (20), formulated for a single monovalent ionic species, predicts C_m dependency on membrane potential and ionic charge. Although the dependency of C_m on ion valency found in this work may, in some cases, be of the same order of magnitude as that predicted by Eq. (20), C_m was found to be practically independent of E_m ($\Delta\psi$ in Eq. (20)) over a wide range (± 200 mV). However, prolonged depolarization of the membrane beyond $E_m = -20$ mV resulted in a large change in C_m. As this change was accompanied by a large increase in leakage current, one may assume that it reflects a major change in the membrane structure. The small changes in membrane dielectric constant with electric fields varying from zero to about 10^5 V/cm is in agreement with the small changes (1 to 5%) of ε of most dielectrics in this range (Smyth, 1955).

From the above discussion, one may conclude that the capacitive properties of the giant axon membrane are primarily the result of the dielectric behavior of the membrane matrix, most probably the lipid phase. The membrane structure as reflected by its dielectric behavior seems to be very stable, and it is only slightly altered by large changes in the ionic composition of the medium, membrane potential field, or temperature.

This investigation was supported by U.S. Public Health Service Grant NB 04601 and by U.S. Public Health Service International Postdoctoral Research Fellowship 1F05TW01220.

References

Adelman, W. J., Palti, Y. 1969. The influence of external potassium on the inactivation of sodium currents in the giant axon of the squid, *Loligo pealei*. *J. Gen. Physiol.* **53**:685.

Chandler, W. K., Meves, H. 1965. Voltage clamp experiments on internally perfused giant axons. *J. Physiol.* **117**:500.

Cole, K. S. 1949. Dynamic electrical characteristics of the squid axon membrane. *Arch. Sci. Physiol.* **3**:253.

— 1968. Membranes, Ions and Impulses. Univ. of Calif. Press, Berkeley.

Curtis, H. J., Cole, K. S. 1938. Transverse electric impedance of the squid giant axon. *J. Gen. Physiol.* **21**:757.

Decker, A. J. 1959. Solid State Physics. Prentice-Hall, Inc., Englewood Cliffs, N.J.

Fishman, H. J., Cole, K. S. 1969. On line measurement of squid axon current potential characteristics. *Fed. Proc.* **28**:333.

FitzHugh, R. 1960. Thresholds and plateaus in the Hodgkins-Huxley nerve equations. *J. Gen. Physiol.* **43**:867.

Hanai, T., Haydon, P. A., Taylor, J. 1965. Polar group orientation and the electric properties of lecithin bimolecular leaflets. *J. Theoret. Biol.* **9**:278.

Hodgkin, A. L., Huxley, A. F. 1952*a*. Currents carried by sodium and potassium ions through the membrane of the giant axon of Loligo. *J. Physiol.* **116**:449.

— — 1952*b*. The components of membrane conductance in the giant axon of Loligo. *J. Physiol.* **116**:473.

— — 1952*c*. A quantitative description of membrane current and its application to conduction and excitation in nerve. *J. Physiol.* **117**:500.

Mauro, A. 1962. Space charge regions in fixed charge membranes and the associated property of capacity. *Biophys. J.* **2**:179.

Palti, Y., Adelman, W. J. 1969. Voltage clamp measurements of membrane conductance and capacity by oscillating potential control. *Fed. Proc.* **28**:333.

Ralston, A., Wilf, H. S. 1960. Mathematical Methods for Digital Computers. John Wiley and Sons, Inc., New York.

Schwan, H. P. 1965. Biological impedance determinations. *J. Cell. Comp. Physiol.* **66** (Suppl. **2**):5.

Small, D. M. 1967. Phase equilibria and structure of dry and hydrated egg lecithin. *J. Lipid Res.* **8**:551.

Smyth, C. P. 1955. Dielectric Behavior and Structure. McGraw-Hill Book Co., Inc., New York.

Spiegel, M. R. 1963. Theory and Problems of Advanced Calculus. Schaum Publ. Co., New York.

Taylor, R. E. 1965. Impedance of the squid axon membrane. *J. Cell. Comp. Physiol.* **66** (Suppl. **2**):21.

Taylor, R. E., Chandler, W. K. 1962. Effects of temperature on squid giant axon membrane capacity. *Biophys. Soc. Abstr.* TD 1.